NEOPLASIA
www.neoplasia.com

Volume 21 Number 4 April 2019 pp. 343–352 343

ErbB3 Ligand Heregulin1 Is a Major Mitogenic Factor for Uncontrolled Lung Cancer Cell Proliferation[1,2]

Shiqi Ma[*,3], Shijun Jia[†,3], Yuan Ren[*], Bangrong Cao[*], Xiao Zha[*], Jintao He[‡] and Changmin Chen[*,§]

[*]Department of Basic Research, Chengdu, Sichuan, 610000; [†]Department of Pathology, Chengdu, Sichuan, 610000; [‡]Department of Thoracic Surgery, Sichuan Cancer Hospital/Institute, Chengdu, Sichuan, 610000; [§]Sichuan Precision Medicine Technology Co., Ltd, Chengdu, Sichuan, 610000

Abstract

There are seven ligands for the epidermal growth factor receptor (EGFR) ErbB1 and two ligands for ErbB3. EGFR can form a homodimer or a heterodimer with ErbB3. In this study, we investigated whether homodimers or heterodimers, and which ligand, play a major role in cancer development, with the goal of ultimately identifying therapeutic targets. We demonstrated that the ErbB3 ligand heregulin1 is the strongest mitogenic factor for non–small cell lung cancer cells and is more potent in activating EGFRmut-ErbB3 heterodimers than EGFRwt-ErbB3 heterodimers. We discovered that four of the seven EGFR ligands inhibited heregulin1-induced EGFRwt-ErbB3 activation and cell proliferation by promoting dephosphorylation of heregulin1-induced ErbB3 phosphorylation, whereas the other three did not exhibit such inhibition. Importantly, those four EGFR ligands did not inhibit heregulin1-induced EGFRmut-ErbB3 activation and proliferation of cells with EGFR mutants. We demonstrated that ErbB3 was overexpressed in the lung cancer cells but not in the adjacent normal alveoli or stromal tissue. EGFR and heregulin1 were also highly expressed in lung cancer cells. We conclude that the overexpression of heregulin1, ErbB3, and EGFR mutant renders uncontrolled cell proliferation.

Neoplasia (2019) 21, 343–352

Introduction

The ErbB receptor tyrosine kinase family has four members: EGFR (ErbB1), ErbB2, ErbB3, and ErbB4 [1]. There are seven ligands for EGFR: epidermal growth factor (EGF), transforming growth factor-α (TGF-α), heparin-binding EGF-like growth factor (HB-EGF), betacellulin (BTC), amphiregulin (AREG), epiregulin (EREG), and epigen (EPGN) [2,3]. There are two ligands for ErbB3: heregulin1 (HRG1) and heregulin2 (HRG2), which are the type I and II isoforms of neuregulin family (NRG1-4) [4]. The seven EGFR ligands demonstrate different binding affinities to EGFR and can be divided into two groups: EGF, TGF-a, BTC, and HB-EGF with high affinity and the others with low affinity [5,6]. Their capacities to induce EGFR dimerization are also different [7]. Consequently, they induce different biological effects even in the same cell line [7]. Although four of the EGFR ligands have a higher affinity than the other three, the expression levels of the high-affinity ligands are not as high as those of the low-affinity ligands in certain cancer cells [8,9]. As a result, the specific ligand that eventually occupies EGFR on cancer cells is not clear. In addition, EGFR can form a homodimer or a heterodimer with ErbB3 [10], creating further ligand binding complexity. According to the rotation model of EGFR-ErbB3, EGFR and ErbB3 form a heterodimer before the ligands bind [11,12], indicating that both EGFR ligands and ErbB3 ligands could bind to the EGFR-ErbB3 heterodimer simultaneously. The effect on cells by different combinations of EGFR and ErbB3 ligands binding to EGFR-ErbB3 heterodimer is not understood [13].

It is well known that EGFR mutation (EGFRmut) plays an important role in cancer development [14–16]. In non–small cell lung cancer

Address all correspondence to: C. Chen, Sichuan Precision Medicine Technology CO., LTD, Chengdu, Sichuan, 610000.

[1] Financial support: This study was supported by the basic research fund of the science and technology department of Sichuan province of China (2015JY0011 to Chen C. and 2011FZ0112 to He J.).

[2] Conflict of interest: None of the authors have a financial conflict of interest related to this work.

[3] Shiqi Ma and Shijun Jia have contributed equally to the work.

Received 3 October 2018; Revised 31 January 2019; Accepted 4 February 2019

1476-5586
https://doi.org/10.1016/j.neo.2019.02.001

(NSCLC) cells, the deletion of five amino acids (E746-A750del) and point mutation (L858R) of EGFR are associated with the development and maintenance of this disease [17–20]. Although mutations of EGFR increase their kinase activity, the mutants still need ligand stimulation for further activation [4,21]. Currently, it is not clear which ligand is responsible for the initiation and progression of NSCLC with EGFRmut. It is also not clear whether the EGFRmut-EGFRmut homodimer or EGFRmut-ErbB3 heterodimer is the driver for NSCLC development. In this study, we investigated which EGFR ligand or ErbB3 ligand is responsible for NSCLC proliferation. We also investigated the mechanism behind their action.

Materials and Methods

Cell Lines and Materials

All cell lines were obtained from the American Type Culture Collection (ATCC, Manassas, VA) and the cell bank of the Chinese Academy of Sciences (Shanghai, China). The cells were expanded when they arrived. Cells were aliquoted into 20 to 30 vials and kept in liquid nitrogen after being found mycoplasma-free using two test kits (Mycoalert Mycoplasma Detection Kit LT07-218 from Lonza and PCR Mycoplasma Test Kit K0103 from HuaAn). The Cell Counting Kit-8 (CCK8) was purchased from Dojindo (Tokyo, Japan).

The antibodies of anti–phospho-AKT (cat. no. 4060), anti–phospho-ERK1/2 (cat. no. 9101), anti-ERK (cat. no. 9102), anti-HER3/ErbB3 (cat. no. 12708), anti-rabbit IgG (H + L), F(ab')2 Fragment (Alexa Fluor 488) (cat. no. 4412), protein-A agarose beads (cat. no. 9863), and the rabbit polyclonal anti-EGFR antibody (cat. no. 2232) were purchased from Cell Signaling Technology (Danvers, MA). The antibodies of anti-EGFR (cat. no. ab52894), anti-ErBb3 (cat. no. ab20161; cat. no. ab93739), anti-Mouse IgG H&L (Alexa Fluor 647) (cat. no. ab150115), and anti-EGF (cat. no. ab9695) were purchased from Abcam (Cambridge, MA). The antibodies of anti-Betacellulin (cat. no. bs-12864R) and anti-Epigen (cat. no. bs-5767R) were purchased from Bioss (Beijing, China). The antibodies of anti-HB-EGF (cat. no. AF-259-NA), anti-epiregulin (cat. no. AF1195), anti-HRG1-β1 (cat. no. AF-396-NA), anti-amphiregulin (cat. no. AF262), and anti-TGFα (cat. no. AF-239-NA) were purchased from R&D (Minneapolis, MN). Anti-Rabbit IgG F(ab') 2 fragment-Atto488 (cat. no.36098); 4′,6-diamidino-2-phenylindole dihydrochloride (DAPI) (cat. no. 28718–90-3); and Puromycin (cat. no. P8833, Herxadimethrinebromidc (cat. no. 107689) were purchased from Sigma-Aldrich (St. Louis, MO). The secondary antibody of rabbit lgG (cat. no. HA1001) was purchased from HuaAn BIO (Hangzhou, China).

EGF (cat. no.AF-100-15), TGFα (cat. no.100-16A), Amphiregulin (cat. no. 200-55B), Epiregulin (cat. no. 100-04), Betacellulin (cat. no. 100-50), Epigen (cat. no. 100-51), HB-EGF (cat. no.100-47), HRGβ1 (cat. no. 100-03), and Murine IL-3 (cat. no. 213-13) were purchased from PeproTech (Rocky Hill, NJ). HRGβ2 (cat. no. CYT-407) was purchased from Prospec (Israel).

An RNeasy Minikit (cat. no. 74104), a PCR Purification kit (cat. no. 28104), a Gel Extraction Kit (cat. no. 28706), and a Plasmid Maxi kit (cat. no. 12162) were purchased from QIAGEN (Hilden, Germany). A Superscript III First-Strand synthesis system for RT-PCR (cat. no. 18080-051) and all tissue culture mediums were purchased from Invitrogen Life Technologies (Carlsbad, CA). All restriction enzymes were purchased from New England Biolabs (Ipswich, MA). ErbB3 full-length cDNA (cat. no. HG10201-M) was purchased from Sino Biological (Beijing, China). Neomycin (cat. no. 10131-055) and OPTI-MEM (cat. no. 31985-062) were purchased from Gibco (Grand Island, NY). X-treme GENE HP DNA Transfection Reagent (cat. no. 06366236001) was purchased from Roche (Mannheirn, Germany). The lentiviral expression vectors pL-tdTomato-Luc-Neo and FUW-Luc-mCH-puro were kind gifts from Dr. Jun Du of Sun Yat-sen University (China).

Construction of EGFR and ErbB3 Expression Vectors

RNA was extracted using an RNeasy Minikit from A549 cells expressing EGFRwt and HCC827 cells expressing EGFRmut. The cDNA was synthesized with the Superscript III First-Strand synthesis system. The full lengths of the EGFRwt and EGFRmut were amplified by two rounds of PCR using Phusion high-fidelity DNA polymerase. The EGFR fragments were cloned into FUW-Luc-mCH-puro plasmid at the XbaI and BstBI sites to generate FUW-EGFR-mCH-puro lentiviral expression plasmids. The first round of amplification primers was as follows:

Primer 1: 5′-tcgactctagaggatccgccaccatgcgaccctccgggacggccggg-3′
Primer 2: 5′-ggccagcttcagcagggcgtagttggtgcactggccggagcctgctccaa-taaattcactgctttgtg-3′.

The second round of amplification primers was as follows:

Primer 1: 5′-tcgactctagaggatccgccaccatgcgaccctccgggacggccggg-3′
Primer 2: 5′-ccatttcgaaagggccagggttgctctccacgtcgccggccagcttcag-cagggcgtag-3′.

ErbB3 was amplified by PCR using human ErbB3 cDNA as a template. ErbB3 was cloned into the pL-tdTomato-Luc-Neo plasmid at the Xbal and EcoRI sites to generate pL-tdTomato-ErbB3-Neo lentiviral expression plasmid. The PCR primers for amplifying ErbB3 were as follows:

Primer 1: 5′-atactctagaatgagggcgaacgacgctctg-3′
Primer 2: 5′-caattgatatccgttctctgggcattagcctt-3′.

Establishment of IL-3–Dependent Bone Marrow Cells (BM-IL-3)

A BALB/c mouse was euthanized in a CO_2 chamber. Its femur was removed. After cutting both ends of the femur, bone marrow cells were flushed out into a 10-cm dish. After being washed with PBS, the cells were incubated with medium containing 10% serum, IL-3 at 50 ng/ml, and FDC-P1 conditioned medium until IL-3–dependent cells were obtained.

Establishment of Stable Cells

CHO cells, FDCP1, and BM-IL-3 cells were mixed with FUW-Luc-mCH-puro, pL-tdTomato-ErbB3-Neo lentivirus, or both, and polybrene at 10 μg/ml. Twenty-four hours after the transfection, the medium was replaced with 10 ml of fresh growth medium containing puromycin at 2.5 μg/ml, neomycin at 500 μg/ml, or both antibiotics. The cells were incubated under selection until puromycin or neomycin-resistant cells were obtained.

Cell Proliferation Assays

FDC-P1 and BM-IL-3 cells were washed three times to remove IL-3 and were seeded in 96-well plates at 4000 cells/well in 100 μl of 5% FBS medium and then treated with EGFR, ErbB3 ligands,

or both at 20 ng/ml for 0, 24, 48, 72, and 96 hours. NSCLC cells were seeded in 96-well plates at 4000 cells/well in 100 μl of 0.1% FBS medium and then were treated with EGFR and ErbB3 ligands at 20 ng/ml for 72 hours. The relative cell number was determined with CCK8 by following the manufacturer's instruction: 10 μl of the CCK8 was added into each well. The plates were incubated at 37°C for 2 hours. The OD value at 450 nm was measured with an iMark microplate reader from Bio-Rad.

Immunofluorescence Assays of EGFR Nuclear Translocation

Cells were grown on 14-mm glass coverslips in 24-well plates and then were serum-starved overnight. The next day, EGFR and ErbB3 ligands at 50 ng/ml were added to cells for 30 minutes. The cells were washed three times with ice-cold PBS and fixed with 4% para-formaldehyde for 15 minutes at room temperature. After being washed three times with PBS, cells were permeabilized with ice-cold PBS containing 0.25% Triton-X100 for 5 minutes. Then, cells were incubated with 10% bovine serum albumin for 1 hour after being washed three times with PBS. Anti-EGFR antibody was incubated with the cells overnight at 4°C. The cells were washed three times and incubated with an Alexa488-conjugated anti-rabbit secondary antibody for 1 hour. Cells were then washed three times with PBS and one time with MilliQ water. After the nuclei were stained with DAPI at 5 μg/ml for 5 minutes, the cells were washed three times with PBS, and the coverslips were removed and put on glass slides with antifluorescence quencher. Pictures were taken with a 100× oil lens on a Nikon A1 Laser Scanning Confocal Microscope.

STORM Imaging Analysis of EGFR-ErbB3 Interaction

Cells were seeded on the glass bottom culture dishes. Growth factors at 20 ng/ml were added to the cells for 15 minutes. The cells were washed three times with ice-cold PBS and fixed with 4% para-formaldehyde for 15 minutes at room temperature. After being washed three times, the cells were permeabilized with ice-cold PBS containing 0.25% Triton-X100 for 5 minutes. Anti-EGFR antibody and anti-ErBb3 antibody were added to the cells for 1 hour at room temperature. The cells were washed three times and incubated with Atto-488-conjugated anti-rabbit secondary antibody and Alexa Fluor 647-conjugated anti-mouse secondary antibody for 30 minutes. The cells were washed three times and fixed with 4% para-formaldehyde again for 10 minutes. STORM imaging was performed with an N-STORM system built on a Nikon-Ti-E inverted microscope with an HP Apo 100× TIRF objective with a numerical aperture of 1.49. Fluorescent images were collected using a HAMAMATSU ORCA-Flash4.0 V2 camera running at a frame rate of 100 fps. Samples were imaged for 30,000 frames in a freshly prepared buffer (50 mM Tris-HCl, pH 8.0, 50 mM NaCl, 10% glucose, 1% 2-mercaptoethanol, 35 μg/ml catalase, and 560 μg/ml glucose oxidase). The 3D STORM image was reconstructed using algorithms for molecule identification and drift correction employed by Nikon Instruments. The Pearson's correlation was calculated by Nikon NIS Elements image analysis software to reflect the level of protein colocalization in each group.

Immunoprecipitation

Cells were serum-starved for 24 hours and then were treated with PBS, EGF, HRG1, and HRG1 plus EGF at 20 ng/ml for 15 minutes, respectively. All cells were harvested and lysed in a NP-40 buffer containing phosphatase inhibitors. Two hundred microliters of cell lysate was preincubated with 20 μl of protein-A agarose beads on a rotator for 1 hour at 4°C. The mixtures were centrifuged at 3000 rpm at 4°C. The supernatants were moved into a new tube and incubated with rabbit polyclonal anti-EGFR antibody overnight at 4°C with rotation. Twenty microliters of protein A agarose beads was added into the mixture and incubated on a rotator for 3 hours at 4°C. Beads were centrifuged down with 3000 rpm at 4°C and washed with 500 μl of NP-40 buffer for 10 minutes at 4°C with rotation. After being washed three times, the beads were resuspended in 20 μl of 2× loading buffer. The resulting samples were boiled for 15 minutes and centrifuged at 3000 rpm for 10 seconds at room temperature. The supernatant was used for SDS/PAGE electrophoresis. Blots were probed with rabbit monoclonal anti–ErbB-3 antibody.

Immunohistochemistry (IHC)

Tumor tissues were fixed in 4% polyoxymethylene, embedded in paraffin, sectioned to 3-μm pieces, and mounted on adhesion microscope slides. Deparaffinization and rehydration were performed in the following standard procedure. Antigen retrieval was performed by boiling slides in EDTA buffer (pH 9) for 20 minutes, and the slides were cooled on bench top for 20 minutes. The activity of endogenous peroxidases was quenched by incubation in 3% H_2O_2 for 10 minutes at room temperature. After being washed with PBS three times, the slides were then incubated with primary antibodies at 4°C overnight. The slides were equilibrated to room temperature for 1 hour. Slides were washed with PBS three times for 5 minutes. Secondary antibodies were added to slides and incubated for 1 hour. After being washed three times, slides were visualized using diaminobenzidine as a chromogenic substrate for 2 minutes and counterstained with hematoxylin for 2 minutes. Differentiation was performed using 1% HCl in 75% ethanol for 30 seconds. Quantitative analysis of ligand expression levels between tumor and nontumor cells was performed by TissueGnostics Asia Pacific Limited. The slides were scanned by a TissueFAXS Plus system (TissueGnostics GmbH) and analyzed by StrataQuest.

Real-Time PCR

Real-time PCR was performed with 200 ng of RNA on a CFX-Connect Real-time PCR Detection System with iTaq Universal SYBR One-Step Kit. The primer sequences were:

EGFR forward primer, 5′-TCCAAGCTGTCCCAATGGGAG-3′, and reverse primer, 5′-GGGCACAGATGATTTTGGTCA-3′;
ErbB3 forward primer, 5′-AGGTGGGCAACTCTCAGGCAG-3′, and reverse primer, 5′-GTCTGGTATTGGTTCTCAGCA-3′;
EGF forward primer, 5′-CAG AAGATGACACTTGGGAGC-3′, and reverse primer, 5′-TGCTGCTGCAGTTTCCTTTCC-3′;
TGF-α forward primer, 5′-CACCGCCTTGGTGGTGGTCTC-3′, and reverse primer, 5′-CAGTGTTTTCGGACCTGGCAG-3′;
AREG forward primer, 5′-ATCCATGTAATGCAGAATTTC-3′, and reverse primer, 5′-TCACCGAAATATTCTTGCTGA-3′;
EREG forward primer, 5′-TGGACATGAGTCAAAACTACT-3′, and reverse primer, 5′-GAAGTGTTCACATCGGACACC-3′;
BTC forward primer, 5′-ACCCTGAGGAAAACTGTGCAG-3′, and reverse primer, 5′-CTTGTATTGCTTGGGGCACCT-3′;
HRG1 forward primer, 5′-GAGAATGTCCAGCTGGTGAAT-3′, and reverse primer, 5′-GAAGTATAGTGACTGGTGGA A-3′.

The fold expression was calculated as follows: fold expression = $2^{\text{cq value of GAPDH-cq value of receptors}}$ or = $2^{\text{cq value of EGF-cq value of ligand}}$. Relative fluorescence units (RFUs) from eight amplification cycles postthreshold

were used to evaluate the amplification efficiency for each pair of primers.

Results

Heregulin 1-the Major Mitogenic Factor for NSCLC Cells

All lung cancer cell lines do not depend on a single EGFR ligand. They also produce multiple EGFR and ErbB3 ligands, which make it challenging to parse out the effect of individual ligands. To investigate which ligand is responsible for cell proliferation, we created cells that are dependent on EGFR and ErbB3 ligands for proliferation. We stably expressed both EGFR and ErbB3 on IL-3–dependent murine myeloid FDC-P1 cells. Before being exposed to EGFR and ErbB3 ligands, these cells were maintained in a medium containing IL-3. After removal of IL-3, the cells were exposed to different ErbB3 and EGFR ligands. As shown in Figure 1, HRG1 is the strongest mitogenic factor for EGFR-ErbB3 expressing FDC-P1 cell proliferation. The cell number treated with HRG1 is two times to six times more than when treated with other ligands (Figure 1, *A* and *B*). When we compared the effect of HRG1 on heterodimers of EGFRmut-ErbB3 and EGFRwt-ErbB3, we found that HRG1 stimulated 1.4 times more growth in the EGFRmut-ErbB3–expressing FDC-P1 cells than in EGFRwt-ErbB3–expressing FDC-P1cells (Figure 1*C*). As a control, IL-3 induced proliferation of both EGFRwt-ErbB3– and EGFRmut-ErbB3–expressing FDC-P1 cells equally (Figure 1*D*). These results demonstrate that HRG1 prefers to activate EGFRmut-ErbB3 over EGFRwt-ErbB3 and is the strongest factor for EGFR-ErbbB3 heterodimer activation. HRG2 also prefers to activate EGFRmut-ErbB3 over EGFRwt-ErbB3 but with less potent mitogenic activity (Supplemental Data 1*A*). To confirm that HRG1 induced proliferation of EGFR-ErbB3–expressing FDC-P1 cells through an EGFR-ErbB3 heterodimer, the cells expressing either ErbB3 or EGFR alone were treated with ErbB3 ligands EGF and IL-3. The cells expressing either ErbB3 or EGFR alone did not respond to HRG1 and HRG2 but responded to IL-3, and cells expressing EGFR responded to EGF and IL-3 (Supplemental Data 1*B*). These results demonstrate that HRG1 and HRG2 acted through an EGFR-ErbB3 heterodimer in these cells. Interestingly, three EGFR ligands (AREG, EREG, and EPGN) prefer to activate EGFRmut over EGFRwt as well (Supplemental data 1*C* upper panel), although their overall mitogenic activities are very weak. However, the other four EGFR ligands (EGF, TGF-α, BTC, and HB-EGF) equally induced proliferation of both EGFRwt-ErbB3– and EGFRmut-ErbB3–expressing FDC-P1 cells (Supplemental data 1*C* lower panel). In addition, we made IL3-dependent cells from BALB/c mouse bone morrow (BM cells) and stably expressed both EGFR and ErbB3 on these cells. Both EGFR-ErbB3–expressing BM cells and EGFR-ErbB3–expressing FDC-P1 cells, either EGFRwt-ErbB3 or EGFR mut-ErbB3, demonstrated the same characteristics in response to all EGFR and ErbB3 ligands (Supplemental Data 2). Finally, we investigated the effect of these ligands on the proliferation of NSCLC cells HCC827 with EGFR containing E740-A750del and H1975 with EGFR containing L858R point mutation. HCC827 and H1975 cells were incubated with 0.5% serum and individual ligands for 72 hours. Since the proliferation of these cells was weak under these conditions, the difference between treatments was not significant. However, when we just compared the differences above the level of nontreatment control, we repeatedly observed that, among the EGFR and ErbB3 ligands, HRG1 is the strongest mitogenic factor for lung cancer cells with EGFRmut

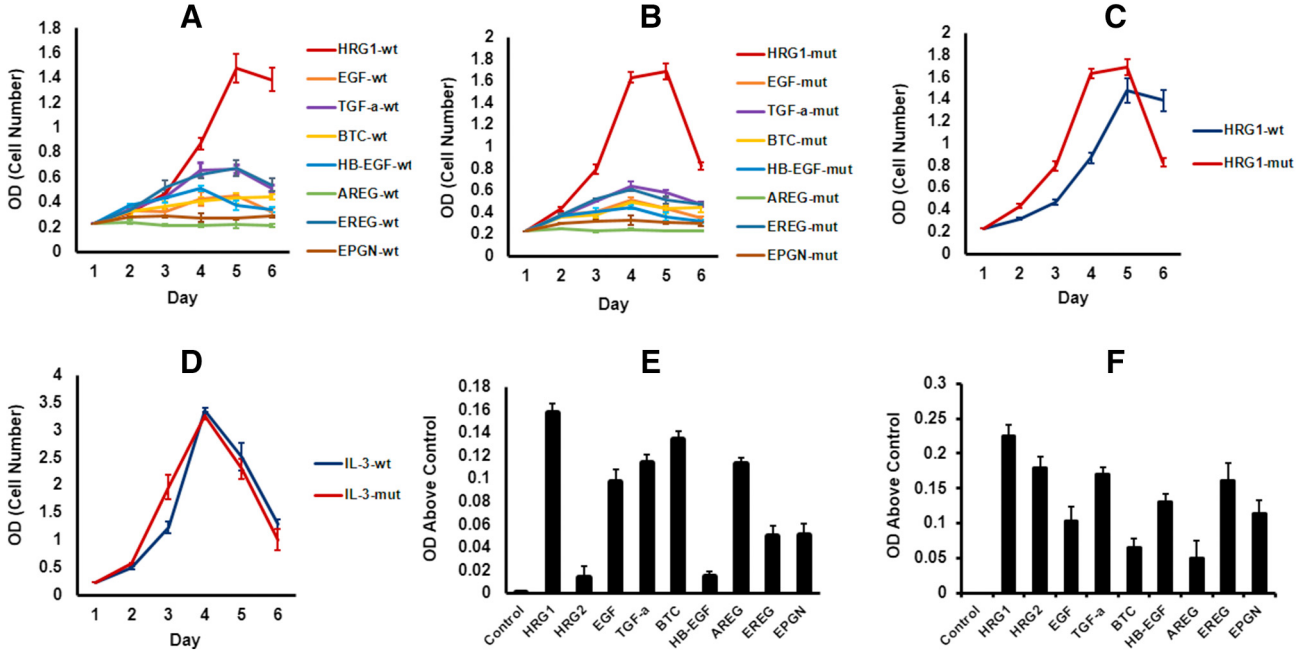

Figure 1. Heregulin1 is the major mitogenic factor for cell proliferation: (A-D) EGFR-ErbB3–expressing FDC-P1 cells were seeded in 96-well plates and treated with different EGFR and ErbB3 ligands or IL-3 at 20 ng/ml at different times. (E-F) NSCLC cells were seeded in 96-well plates and were treated with EGFR and ErbB3 ligands at 20 ng/ml for 72 hours. The relative cell number was determined with CCCK8. The OD value at 450 nm was measured with an iMark microplate reader. Results were shown as cell growth curves for EGFRwt-ErbB3– and EGFRmut-ErbB3–expressing FDC-P1 cells in response to ligand stimulation, respectively (A-D). The difference above the nontreatment control was compared in order to determine which ligand was the major mitogenic factor for NSCLC cells with EGFRmut (E-F). Data are plotted as mean +/− SD of tetraplicates. The data are representative of three independent experiments.

(Figure 1, *E* and *F*). The relative expression level of ErbB3 and EGFR of these cells is shown in Supplemental data 3.

EGF, TGF-α, BTC, and HB-EGF-Inhibitory Factors on HRG1-Induced Proliferation of Cells with EGFRwt-ErbB3, But Not with EGFRmut-ErbB3

Since both EGFR ligands and ErbB3 ligands can bind to an EGFR-ErbB3 heterodimer simultaneously, we investigated the effect of the combination of HRG1 and EGFR ligands on cell proliferation. Surprisingly, EGF, TGF-α, BTC, and HB-EGF inhibited HRG1-induced EGFRwt-ErbB3 cell proliferation (Figure 2*A*), whereas with EGFRmut-ErbB3–expressing cells, they had no inhibition on HRG1-induced cell proliferation. In fact, HRG1 plus EGF or TGF-α and BTC promoted more cell growth, indicating an additive effect on proliferation between them (Figure 2*B*). AREG, EREG, and EPGN did not inhibit HRG1-induced EGFRwt-ErbB3–expressing cell proliferation. They also had additive effects on the proliferation of EGFRmut-ErbB3–expressing cells (Figure 2, *C* and *D* and Supplemental Data 2, *E-H*). We further examined the combined effect of these ligands on lung cancer cells. HRG1 plus EGFR ligands demonstrated a stronger cell proliferation effect on HCC827 cells than HRG1 alone (Figure 2*E*), and EGF inhibited HRG1 induced-proliferation of A549 cells with EGFRwt (Figure 2*F*), similar to the results of FDC-P1 cells with EGFRmut-ErbB3 and EGFRwt-ErbB3 induced by HRG1 plus these ligands.

Mechanism of EGF Inhibiting HRG1-Induced EGFRwt-ErbB3 Heterodimer Activation

We investigated the mechanism of EGF inhibiting HRG1-induced EGFRwt-ErbB3–expressing cell proliferation. As shown in Figure 3*A*, EGF induced Erk1/2 phosphorylation but not ErbB3 phosphorylation, whereas HRG1 induced ErbB3 phosphorylation but not Erk1/2 phosphorylation in both A549 and HCC827 lung cancer cells (Figure 3, *A* and *B*). ErbB3 does not have kinase activity and is phosphorylated by EGFR [22], confirming that EGFR in the EGFR-ErbB3 heterodimer activated by HRG1 is different from that induced by EGF. When cells were treated with both EGF and HRG1, phosphorylation of ErbB3 was inhibited in A549 cells, which express EGFR wild type (Figure 3*A*), but not in HCC827 cells, which express EGFR mutant (Figure 3*B*), suggesting a conformational change of EGFR mutant still allows EGFR to phosphorylate ErbB3 in response to HRG1 binding but hinders its ability to inhibit ErbB3 phosphorylation in response to EGF binding. AREG also induced Erk1/2 phosphorylation (Figure 3*C*) but did not inhibit HRG1-induced ErbB3 phosphorylation in either A549 or HCC827 cells (Figure 3, *C* and *D*), confirming that EGFR induced by AREG is different from that induced by EGF, possibly due to the fact that AREG only induced about half as much total dimerization as EGF did [7]. The same phenomena have also been observed in EGFRwt-ErbB3– and EGFRmut-ErbB3– expressing FDC-P1 cells (Figure 3, *E-H*). TGF-α, but not EREG, also inhibited HRG1-induced ErbB3 phosphorylation in A549 cells (Figure 3*I*).

Recent research has shown that EGFR tends to form a homodimer in the presence of EGF [10]. We investigated whether EGF inhibits HRG1-induced ErbB3 phosphorylation by inducing the EGFR-EGFR homodimer to prevent EGFR from forming a heterodimer with ErbB3. We performed immunofluorescence staining and analyzed them with an N-STORM system. As shown in Figure 4*A*, without ligand treatment, both ErbB3 and EGFR are mainly expressed on the cell membrane. The 3D STORM images of the EGFR-ErbB3 heterodimer were observed on the membrane (Figure 4*B*). EGF, HRG1, and HRG1 plus EGF treatment all resulted in both ErbB3 and EGFR

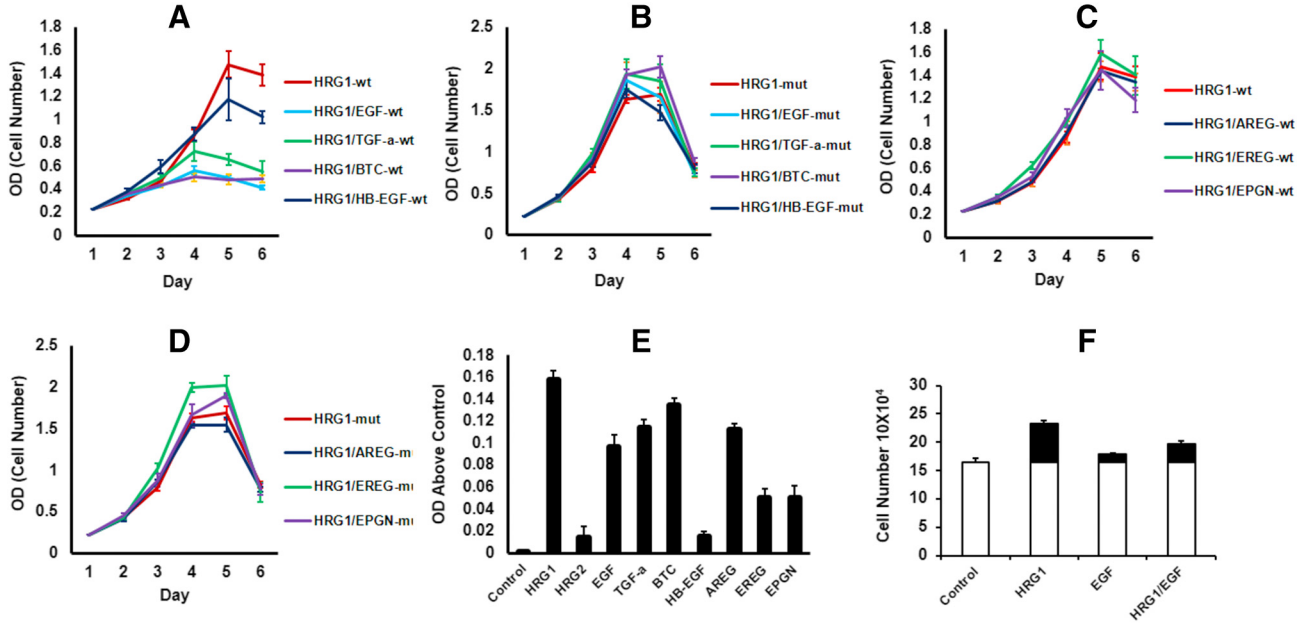

Figure 2. EGF, TGF-a, BTC, and HB-EGF are inhibitory factors on HRG1-induced proliferation of cells with EGFRwt-ErbB3 but not with EGFRmut-ErbB3: (A-D) EGFR-ErbB3–expressing FDC-P1cells were seeded in 96-well plates and treated with different EGFR and ErbB3 ligands at 20 ng/ml at different times. (E-F) NSCLC cells were seeded in 96-well plates and were treated with EGFR and ErbB3 ligands at 20 ng/ml for 72 hours. The relative cell number was determined with CCK8. The OD value at 450 nm was measured with an iMark microplate reader. Results were shown as cell growth curves for EGFRwt-ErbB3– and EGFRmut-ErbB3–expressing FDC-P1 cells in response to different combinations of EGFR and ErbB3 ligand treatment respectively (A-D). The difference above the nontreatment control was compared to show the effect of HRG1 vs. HRG1 plus EGFR ligand treatment for NSCLC cells (E-F). Data are plotted as mean ± SD of tetraplicates. The data are representative of three independent experiments.

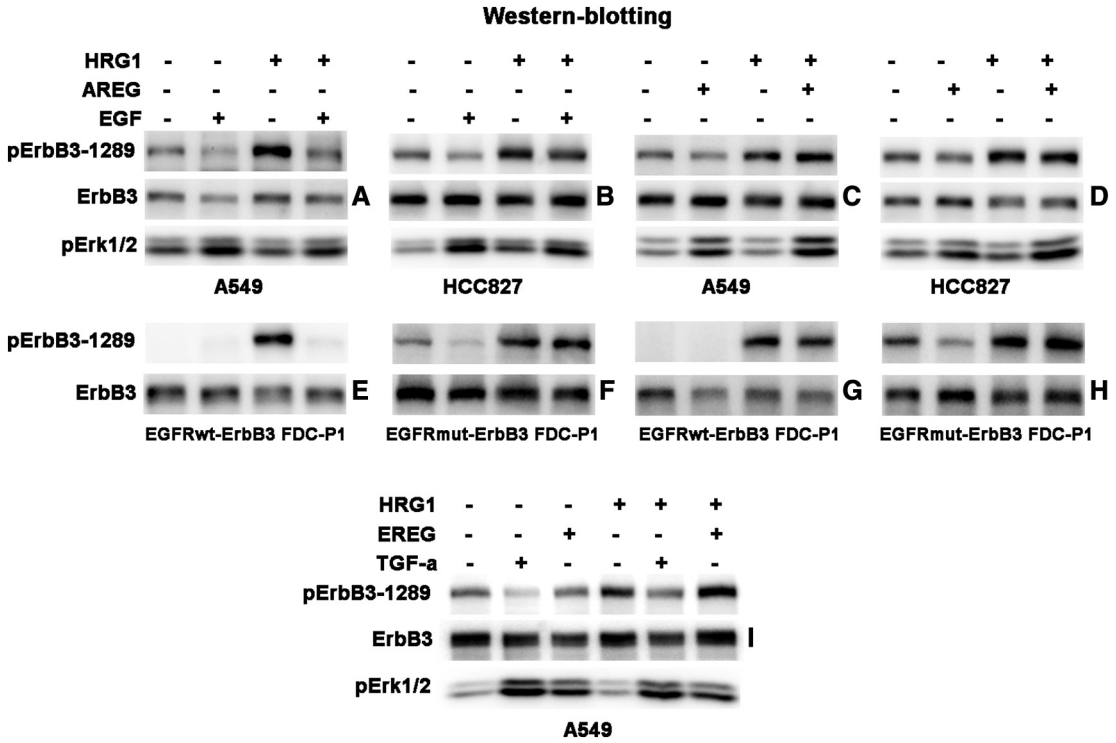

Figure 3. EGF and TGF-α inhibit HRG1-induced ErbB3 phosphorylation in EGFRwt-ErbB3 cells but not in EGFRmut-ErbB3 cells: Cells at 50% confluence were serum starved for 24 hours. The cells were untreated or treated with different ligands at 20 ng/ml for 15 minutes. The cell lyses were subjected to SDS-PAGE. Membranes were first probed with anti-pErbB3 antibody. The membranes were stripped and reprobed with anti-ErbB3 antibody as loading control and anti-pErk1/2 antibody. The data are representative of three independent experiments.

internalization (Figure 4, *C-E*), showing that, even in the presence of EGF, treating with HRG1 still leads to EGFR internalization. Many 3D STORM images of the EGFR-ErbB3 heterodimer, like those shown in Figure 4*B*, were observed in the cytoplasm in all three treatments (data not shown). These results demonstrate that there are preexisting EGFR-ErbB3 heterodimers, and EGF cannot prevent formation of EGFR-ErbB3 heterodimers by inducing the EGFR-EGFR homodimer. Furthermore, we carried out co-immunoprecipitation (Co-IP) with EGFR-ErbB3–expressing FDCP-1 cells to confirm the finding that EGF treatment does not interrupt the formation of EGFR-ErbB3 heterodimers. We did not detect any EGFRwt-ErbB3 heterodimers in the cells treated with either EGF or HRG1 but consistently detected EGFRwt-ErbB3 heterodimers in the cells treated with HRG1 plus EGF (Figure 4*F*), indicating the existence of the EGFR-ErbB3 heterodimer in the presence of EGF. This EGFRwt-ErbB3 heterodimer cannot be detected when the anti-ErbB3 antibody is used for IP. On the other hand, the EGFRmut-ErbB3 heterodimer was consistently detected in the samples treated with HRG1 alone or with HRG1 plus EGF (Figure 4*F*), using either anti-EGFR or anti-ErbB3 antibodies for IP. This demonstrates that either HRG1 or EGF alone does not induce any tight interaction of the EGFRwt-ErbB3 heterodimer, which cannot be detected by Co-IP. The presence of both EGF and HRG1 is required for a tight interaction of EGFRwt-ErbB3 heterodimer. The aforementioned results clearly demonstrate that EGF does not induce the EGFR-EGFR homodimer to prevent EGFR from forming a heterodimer with ErbB3 to inhibit HRG1-induced ErbB3 phosphorylation and cell proliferation. Next, we investigated whether EGF treatment led to the dephosphorylation of ErbB3. We treated cells first with HRG1 for either 10 or 14 minutes to induce phosphorylation of ErbB3, and then with EGF for either 1 minute or 5 minutes. Comparing it to HRG1 treatment alone, we still observed the inhibition of ErbB3 phosphorylation (Figure 4*G*). It is likely that EGF treatment leads to the dephosphorylation of ErbB3.

High Expression of EGFR, ErbB3, and HRG1 on NSCLC Cells

The aforementioned data demonstrate that, with EGFR mutation, HRG1 can promote cell proliferation without the inhibition by four of the seven EGFR ligands. Next, we examined whether ErbB3, EGFR, and their ligands are simultaneously overexpressed in the patient samples. Although previous studies had examined the expression of EGFR and some of its ligand in patient samples [23], the focus of those studies was on the percentage of samples expressing these molecules. We analyzed 16 lung adenocarcinoma patient samples from our hospital pathology laboratory. ErbB3 was detected on the cancer cells of all samples and overexpressed on 10 of them. However, it was not detected in the adjacent normal alveoli or stromal tissue. EGFR was strongly expressed on the cancer cells in all the samples but was weakly or not detected in the adjacent normal alveoli or stromal tissue. HRG1 was expressed at a high level in the tumor cells of all samples but only was modestly expressed in the adjacent normal alveoli or stromal tissue. AREG, EREG, EPGN, BTC, and HB-EGF also were highly expressed in the samples (Figure 5*A*, Supplemental Data 4, *A-E*). The quantitative assay by a TissueFAXS Plus system and StrataQuest showed that expressions of AREG and EREG are higher on cancer cells than on nearby normal alveoli (Supplemental Data 5*A*). However, the expression of EGF and TGF-α is lower in cancer cells than on nearby normal alveoli (Supplemental Data 5*A*). Evidently, overexpression of

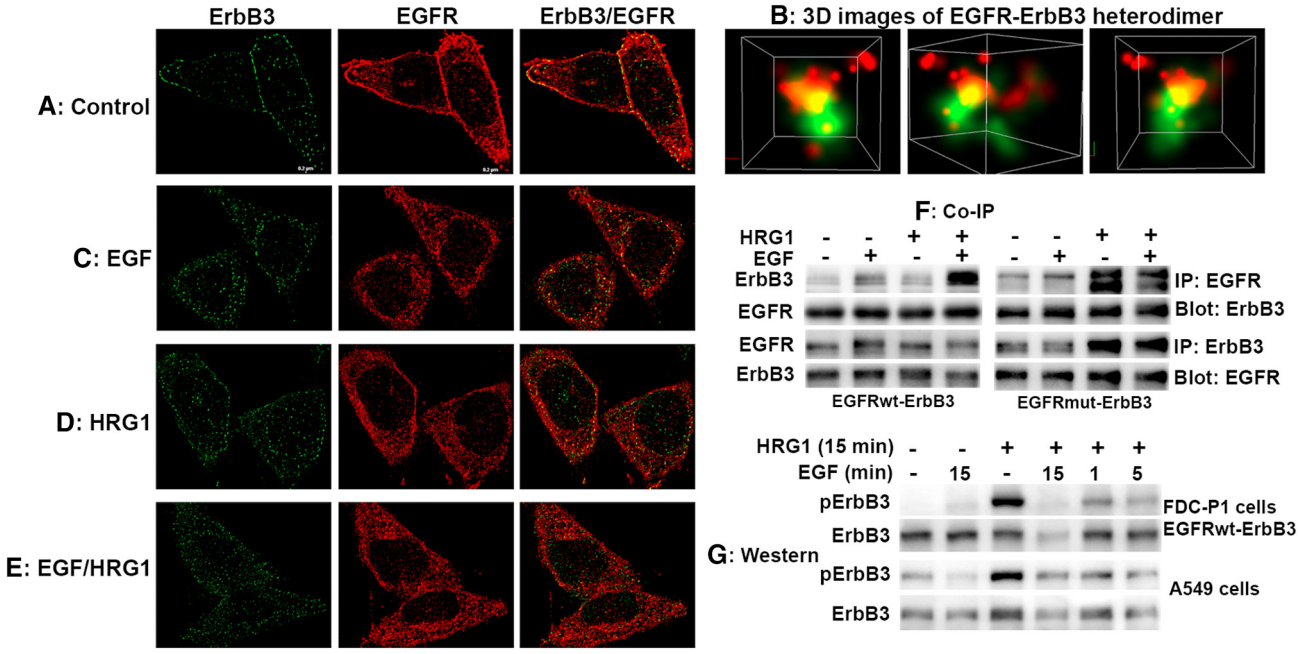

Figure 4. Effect of HRG1 and EGFR ligands on EGFR-ErbB3 heterodimer: (A-E) Imaging analysis of EGFR-ErbB3 heterodimer: Cells were seeded on glass-bottom culture dishes. EGF, HRG1, and HRG1 plus EGF at 20 ng/ml were added to cells for 15 minutes. Cells were immunofluorescence stained. STORM imaging was performed with an N-STORM system built on a Nikon-Ti-E inverted microscope with an HP Apo 100× TIRF objective having a numerical aperture of 1.49. Images demonstrate preexisting EGFR-ErbB3 heterodimers. EGF treatment induced ErbB3 internalization, and HRG1 treatment induced EGFR internalization, respectively. (B) 3D STORM images of EGFR-ErbB3 heterodimer were reconstructed using Nikon NIS Elements image analysis software to reflect the level of protein colocalization. Photos of an EGFR-ErbB3 heterodimer were taken from three different directions. The green color represents ErbB3, and the red color represents EGFR. (F) Co-immunoprecipitation: Cells at 50% confluence were serum starved for 24 hours. The EGFR-ErbB3–expressing FDC-P1 cells were untreated or treated with EGF, HRG1, and EGF plus HRG1 at 20 ng/ml for 15 minutes. The cells were lysed in NP-40 buffer with phosphotase inhibitors. EGFR and ErbB3 were immunoprecipitated and subjected to SDS-PAGE. The membranes were probed with anti-ErbB3 or anti-EGFR antibody. (G) Western blot: Cells were serum starved for 24 hours and were untreated or treated with different ligands for 15 minutes except the last two columns where cells were first treated with HRG1 for 14 or 10 minutes and then treated with EGF for 1 or 5 minutes, respectively (total 15 minutes). Cells lyses were subjected to SDS-PAGE. Membranes were probed antiphosphorylated ErbB3, stripped, and reprobed with anti-ErbB3 antibody as loading contro,l respectively. The data are representative of three independent experiments.

ErbB3, EGFRmut, and HRG1, together with any one of the seven EGFR ligands, leads to the robust proliferation of cancer cells with an EGFRmut-ErbB3 heterodimer.

Discussion

In this study, we created cell models that exhibit dependency on EGFR and ErbB3 ligands for proliferation, allowing us to analyze the effect of an individual ligand on cell proliferation in a "pure" environment. We identified that HRG1 is the major mitogenic factor for the proliferation of these cells and NSCLC cells. HRG1 is a more potent activator for the proliferation of cells with EGFRmut-ErbB3 than cells with EGFRwt-ErbB3, indicating that HRG1 plays an important role in the development and maintenance of NSCLC with EGFRmut. Furthermore, we discovered that four of the seven EGFR ligands (EGF, TGF-α, BTC, and HB-EGF) inhibit HRG1-induced proliferation of cells with EGFRwt but not with EGFRmut. Therefore, when cells overexpress ErbB3, EGFRmut, and HRG1, as shown in the lung cancer patient samples (Figure 5*A*), they cause uncontrolled cell proliferation.

EGF, TGF-α, BTC, and HB-EGF inhibit HRG1-induced proliferation of cells with EGFRwt, indicating that they may play an inhibitory role to prevent HGR1-induced overgrowth of cells with EGFRwt. The mechanism of inhibition by these four ligands on HRG1 induced-cell proliferation has not been understood. According to a recent study, EGFR formed homodimers preferably in the presence of EGF [10]. It is rationally speculated that EGF inhibits HRG1-induced activation by inducing EGFR-EGFR homodimers and preventing the formation of EGFR-ErbB3 heterodimers. However, our immunofluorescence and immunoprecipitation results did not support this speculation since treating cells with EGF led to ErbB3 internalization and treating cells with HRG1 led to EGFR internalization (Figure 4, *C* and *D*). When cells were treated with both EGF and HRG1, EGFR-ErbB3 heterodimer formed tightly (Figure 4*F*), indicating that EGF did not promote the formation of EGFR-EGFR homodimer to interrupt EGFR-ErbB3 heterodimer in order to inhibit HRG1-induced EGFR-ErbB3 activation. Instead, when we first treated cells with HRG1 for either 10 or 14 minutes to induce phosphorylation of ErbB3 and then treated cells with EGF for either 1 minute or 5 minutes, the EGF treatment caused dephosphorylation of ErbB3 in all experiments (Figure 4*G*). We speculated that EGF might activate a phosphatase that dephosphorylated ErbB3. However, when we first stimulated cells with HRG1 and then treated cells with phosphatases inhibitors RK-682 and CAS 765317-72-4, etc., followed by EGF, we still observed that EGF treatment led to dephosphorylation of ErbB3 (data not shown).

The reason why only the four ligands (EGF, TGF-a, BTC, and HB-EGF) can inhibit HRG1-induced EGFR-ErbB3 activation

might relate to the fact that the four ligands have high binding affinity to EGFR [5,6] and induce around two times more total receptor dimerization than the other three ligands can [7]. It is possible that they induce a conformational change of EGFR strong enough to interrupt HRG1 induced-conformational alteration of EGFR-ErbB3. By contrast, the other three ligands induce conformational change of EGFR that is not strong enough to interrupt HRG1 induced-conformational alteration of EGFR-ErbB3. Indeed, we found that EGF, TGF-α, BTC, and HB-EGF have equal effects on the activation of both wild-type and mutant EGFR, indicating that these four ligands might not play a role in the development of lung cancer with EGFR mutation. AREG, EREG, and EPGN activated mutant EGFR as potently as the other four ligands and were able to induce nuclear translocation of EGFR mutant. However, two times the concentration was required for them to activate wild-type EGFR, and they cannot induce nuclear translocation of wild-type EGFR [24] (Supplemental Data 6).

The conformational alteration of EGFR-ErbB3 heterodimer induced by HRG1 is different from that induced by EGF or TGF-α. ErbB3 does not have kinase activity [25,26]. HRG1 binds to the ErbB3 of EGFR-ErbB3 heterodimer and activates EGFR to phosphorylate ErbB3. An EGF- or TGF-α–activated EGFR-ErbB3 heterodimer does not lead to ErbB3 phosphorylation but instead leads to Erk 1/2 phosphorylation and generates weak proliferation signals. Contrastingly, an HRG1-activated EGFR-ErbB3 heterodimer results in ErbB3 phosphorylation, but not Erk1/2 phosphorylation, and generates strong proliferation signals. However, when EGFR contains a five–amino acid deletion (E746-A750del), it loses its capability to inhibit phosphorylation of ErbB3 or dephosphorylate ErbB3 in the NSCLC cells. Therefore, HRG1 plus EGF or TGF-α treatment of EGFRmut-ErbB3 results in the phosphorylation of both ErbB3 and Erk 1/2. This explains why HRG1 plus any one of the seven EGFR ligands induces stronger proliferation in the EGFRmut-ErbB3 cells than HRG1 alone does.

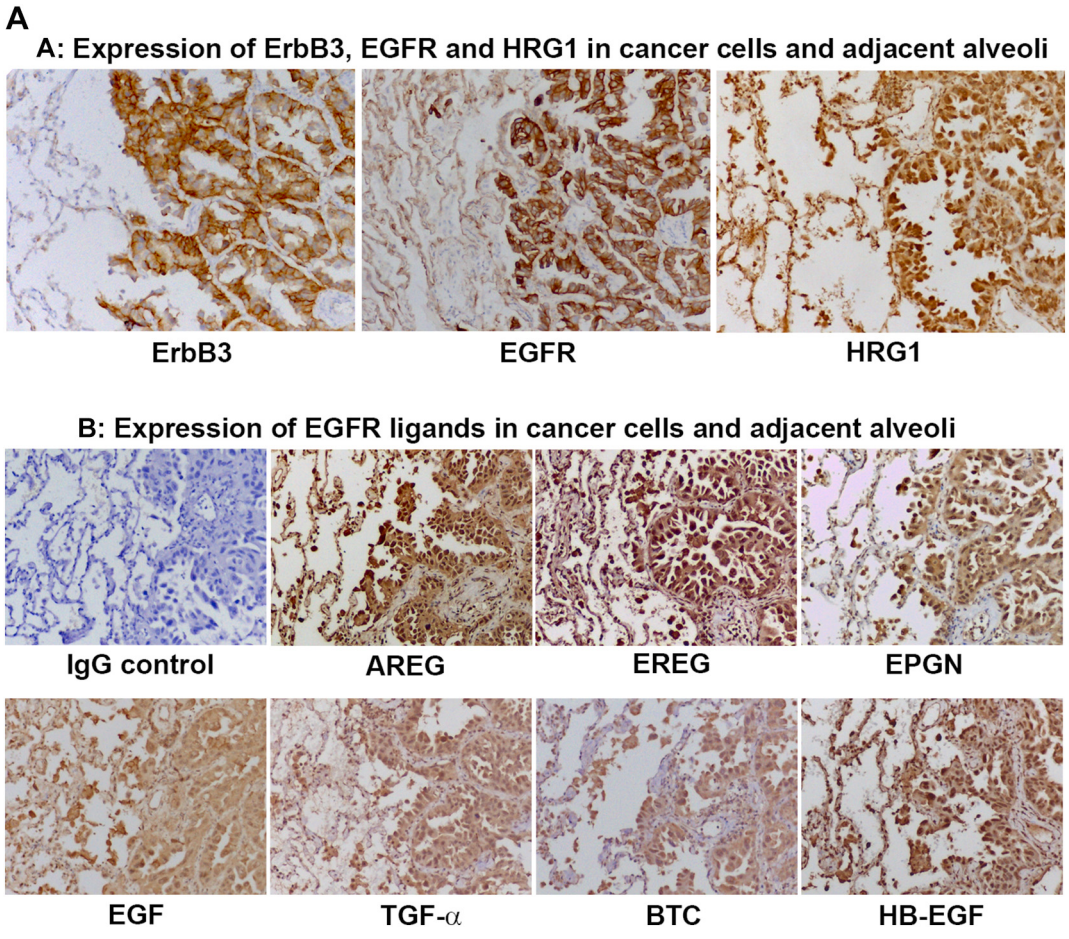

Figure 5. (A) High expression of EGFR, ErbB3, and their ligands: IHC was performed by the following standard procedures of hospital: Pictures were taken at junction area between tumor cells at right side and normal alveoli or stroma tissue at left side with 10×10 amplification from the same one patient with NSCLC harboring EGFR mutant of E746-A750del.(B). Different response to binding of EGFR and ErbB3 ligands: When EGF binds to wild-type or mutant EGFR-ErbB3 heterodimer, the EGFR configuration change allows it to activate MAP kinase pathway and a phosphatase that dephosphorylates ErbB3, which results in a weak proliferation signal (A and E). When HRG1 binds to EGFR-ErbB3 heterodimer, the EGFR configuration change does not allow it to activate MAP kinase pathway but allows it to phosphorylate ErbB3 and generates a strong proliferation signal (B and F). When EGF and HRG1 bind to their receptors simultaneously, the configuration change of wild-type EGFR allows it to activate MAP kinase pathway and activates a phosphatase that dephosphorylates ErbB3, which results in a weak proliferation signal (C), whereas the same event allows mutant EGFR to activate MAP kinase pathway and phosphorylate ErbB3, which results in a stronger proliferation signal (G). When AREG and HRG1 bind to their receptors simultaneously, the configuration change of either wild-type or mutant EGFR allows EGFR to activate MAP kinase pathway and phosphorylate ErbB3, which also results in a stronger proliferation signal (D and H).

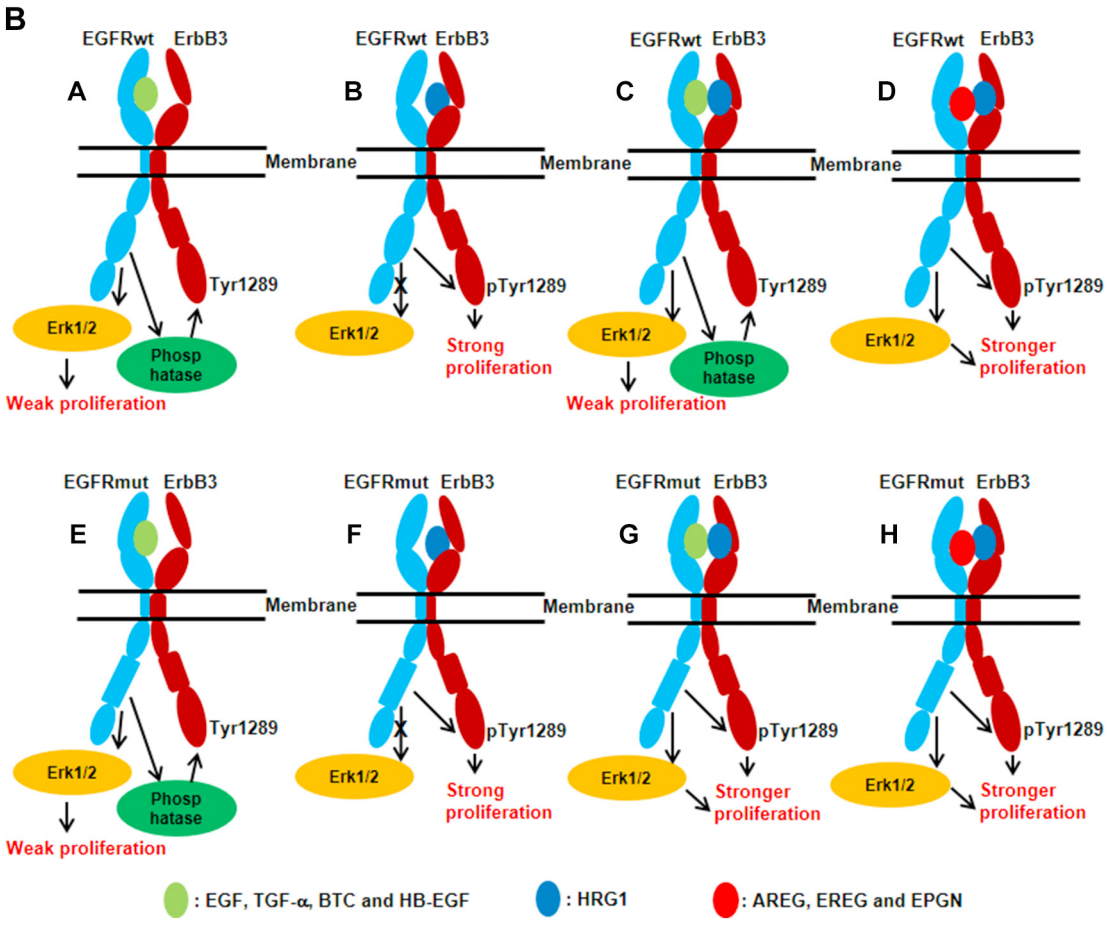

Figure 5 (*continued*).

In addition, AREG or ERRG with a lower affinity to EGFR induces Erk1/2 phosphorylation and does not suppress HRG1-induced ErbB3 phosphorylation in either A549 cells or EGFRwt-ErbB3 expressing FDC-P1 cells, similar to the situation of HRG1 plus EGF-treated EGFRmut-ErbB3 cells. Therefore, AREG or EREG plus HRG1 generates a stronger activation signal than HRG1 does alone and enhances HRG1-induced cell proliferation (Figure 3). The different responses to the binding of EGFR and ErbB3 ligands to their receptors are summarized in Figure 5*B*, from which we propose two mechanisms that drive uncontrolled proliferation of lung cancer cells. The first one is for the cells with EGFR mutation, i.e., the overexpression of EGFR mutant, heregulin1 and ErbB3 render uncontrolled cell proliferation. The second one is for the cells with wild-type EGFR, i.e., high-expression of AREG and EREG, coupled with high expression of EGFR, ErbB3, and heregulin1 and low expression of EGF, TGF-α, and BTC (Supplemental Data 5), excludes the inhibitory effect of the later four EGFR ligands and strongly promotes EGFR wild-type cell proliferation (Figure 5, *B-D* and Supplemental data 7).

Clearly, HRG1-induced ErbB3-EGFR heterodimer activation is an important driver for lung adenocarcinoma, which is consistent with recent studies showing that the cells that survive after chemotherapy overexpress HRG1 [27] and that expression of *CD74-HRG1* fusion gene enhanced cancer initiation [28,29]. Although HRG1 also binds and activates ErbB4, we found that the level of ErbB4 expression was low in several lung cancer cell lines (data not shown). In addition, activation of ErbB4 by HRG1 does not necessarily require ErbB4 to form heterodimer with EGFR mutants that play an important role in the development of lung cancer. Therefore, HRG1-induced ErbB3-EGFR heterodimer activation, rather than HRG1-induced ErbB4 activation, should be the target of pharmaceutical intervention for lung cancer.

ErbB3 does not have kinase activity, and HRG1-activated signaling is achieved by activating EGFR. Therefore, in theory, inhibition of EGFR kinase activity will block the function of HRG1. However, a recent research demonstrated that after treating animal model of EGFR mutant lung cancer cells with the third generation of EGFR inhibitor (osimertinib), cells rapidly developed drug resistance. When combined with anti-EGFR and anti-ErbB2 antibodies, osimeritinib inhibited cancer cells growth without resistance [30]. Possible explanations for why a combination of anti-EGFR and anti-ErbB2 antibodies can overcome resistance of lung cancer to osimertinib are as follows: 1) EGFR wild-type alleles of this cell line are amplified to render cells insensitive to osimertinib [31], and 2) high expression of ErbB2-ErbB3 heterodimer confers cells independent of EGFR-ErbB3 heterodimer. In addition, we found that EGF, TGF-α, and EREG rendered cells resistant to EGFR inhibitors. Interestingly, HRG1 had no effect on EGFR inhibitor-induced cell death (Supplemental Data 8). If the cells overexpress EGF, TGF-α, and EREG, they might rapidly develop drug resistance. Obviously, when lung cancer cells simultaneously express multiple ligands and different level of ErbB receptor tyrosine kinase family members and have different homodimers and heterodimers, inhibition of multiple pathways should be taken into consideration to induce cell apoptosis. However, from a clinical point of view, inhibition of multiple targets might cause severe side effects.

Our study showed that ErbB3 was detected only on lung cancer cells and not in the adjacent normal alveoli or stromal tissue (Figure 5*A*). Therefore, ErbB3 is an ideal therapeutic target for an antibody that is able to activate the complement system and to mediate the antibody-dependent cell-mediated cytotoxicity to lyse the lung cancer cells.

Supplementary data to this article can be found online at https://doi.org/10.1016/j.neo.2019.02.001.

Acknowledgements

Thanks to TissueGnostics Asia Pacific Limited for its professional technical support in image scanning and analysis. Thanks to Mr. Tingqing Chen for preparing lentiviral DNA and Ms. Liping Luo for optimizing antibody concentration for IHC.

References

[1] Burgess AW, et al (2003). An open-and-shut case? Recent insights into the activation of EGF/ErbB receptors. *Mol Cell* **12**(3), 541–552.
[2] Singh B, Carpenter G, and Coffey RJ (2016). EGF receptor ligands: recent advances. *F1000Res* **5**.
[3] Schneider MR and Wolf E (2009). The epidermal growth factor receptor ligands at a glance. *J Cell Physiol* **218**(3), 460–466.
[4] Linggi B and Carpenter G (2006). ErbB receptors: new insights on mechanisms and biology. *Trends Cell Biol* **16**(12), 649–656.
[5] Jones JT, Akita RW, and Sliwkowski MX (1999). Binding specificities and affinities of egf domains for ErbB receptors. *FEBS Lett* **447**(2–3), 227–231.
[6] Ozcan F, et al (2006). On the nature of low- and high-affinity EGF receptors on living cells. *Proc Natl Acad Sci U S A* **103**(15), 5735–5740.
[7] Macdonald-Obermann JL and Pike LJ (2014). Different epidermal growth factor (EGF) receptor ligands show distinct kinetics and biased or partial agonism for homodimer and heterodimer formation. *J Biol Chem* **289**(38), 26178–26188.
[8] Zhang J, et al (2008). Intratumoral epiregulin is a marker of advanced disease in non-small cell lung cancer patients and confers invasive properties on EGFR-mutant cells. *Cancer Prev Res (Phila)* **1**(3), 201–207.
[9] Lemos-Gonzalez Y, et al (2007). Alteration of the serum levels of the epidermal growth factor receptor and its ligands in patients with non-small cell lung cancer and head and neck carcinoma. *Br J Cancer* **96**(10), 1569–1578.
[10] van Lengerich B, et al (2017). EGF and NRG induce phosphorylation of HER3/ERBB3 by EGFR using distinct oligomeric mechanisms. *Proc Natl Acad Sci U S A* **114**(14), E2836-2845.
[11] Littlefield P, et al (2014). Structural analysis of the EGFR/HER3 heterodimer reveals the molecular basis for activating HER3 mutations. *Sci Signal* **7**(354), ra114.
[12] Purba ER, Saita EI, and Maruyama IN (2017). Activation of the EGF receptor by ligand binding and oncogenic mutations: the "rotation model". *Cell* **6**(2).
[13] Wilson KJ, et al (2012). EGFR ligands exhibit functional differences in models of paracrine and autocrine signaling. *Growth Factors* **30**(2), 107–116.
[14] Jorissen RN, et al (2003). Epidermal growth factor receptor: mechanisms of activation and signalling. *Exp Cell Res* **284**(1), 31–53.
[15] Yomo S and Oda K (2018). Impacts of EGFR-mutation status and EGFR-TKI on the efficacy of stereotactic radiosurgery for brain metastases from non-small cell lung adenocarcinoma: a retrospective analysis of 133 consecutive patients. *Lung Cancer* **119**, 120–126.
[16] Paez JG, et al (2004). EGFR mutations in lung cancer: correlation with clinical response to gefitinib therapy. *Science* **304**(5676), 1497–1500.
[17] Sharma SV, et al (2007). Epidermal growth factor receptor mutations in lung cancer. *Nat Rev Cancer* **7**(3), 169–181.
[18] Sakai K, et al (2006). Dimerization and the signal transduction pathway of a small in-frame deletion in the epidermal growth factor receptor. *FASEB J* **20**(2), 311–313.
[19] Rossi S, et al (2016). Different EGFR gene mutations in exon 18, 19 and 21 as prognostic and predictive markers in NSCLC: a single institution analysis. *Mol Diagn Ther* **20**(1), 55–63.
[20] Sasaki H, et al (2006). L858R EGFR mutation status correlated with clinico-pathological features of Japanese lung cancer. *Lung Cancer* **54**(1), 103–108.
[21] Schlessinger J (2000). Cell signaling by receptor tyrosine kinases. *Cell* **103**(2), 211–225.
[22] Bublil EM and Yarden Y (2007). The EGF receptor family: spearheading a merger of signaling and therapeutics. *Curr Opin Cell Biol* **19**(2), 124–134.
[23] Rusch V, et al (1993). Differential expression of the epidermal growth factor receptor and its ligands in primary non–small cell lung cancers and adjacent benign lung. *Cancer Res* **53**(10 Suppl), 2379–2385.
[24] Faria J, et al (2016). Effects of different ligands on epidermal growth factor receptor (EGFR) nuclear translocation. *Biochem Biophys Res Commun* **478**(1), 39–45.
[25] Carraway III KL, et al (1994). The erbB3 gene product is a receptor for heregulin. *J Biol Chem* **269**(19), 14303–14306.
[26] Sierke SL, et al (1997). Biochemical characterization of the protein tyrosine kinase homology domain of the ErbB3 (HER3) receptor protein. *Biochem J* **322** (Pt 3), 757–763.
[27] Hegde GV, et al (2013). Blocking NRG1 and other ligand-mediated Her4 signaling enhances the magnitude and duration of the chemotherapeutic response of non–small cell lung cancer. *Sci Transl Med* **5**(171), 171ra18.
[28] Fernandez-Cuesta L and Thomas RK (2015). Molecular pathways: targeting NRG1 fusions in lung cancer. *Clin Cancer Res* **21**(9), 1989–1994.
[29] Murayama T, et al (2016). Oncogenic fusion gene CD74-NRG1 confers cancer stem cell-like properties in lung cancer through a IGF2 autocrine/paracrine circuit. *Cancer Res* **76**(4), 974–983.
[30] Romaniello D, et al (2018). A combination of approved antibodies overcomes resistance of lung cancer to osimertinib by blocking bypass pathways. *Clin Cancer Res* **24**(22), 5610–5621.
[31] Nukaga S, et al (2017). Amplification of EGFR wild-type alleles in non–small cell lung cancer cells confers acquired resistance to mutation-selective EGFR tyrosine kinase inhibitors. *Cancer Res* **77**(8), 2078–2089.